



University of Kentucky
UKnowledge

Sanders-Brown Center on Aging Faculty
Publications

Aging

11-13-2015

Mice Deficient in Endothelial $\alpha 5$ Integrin are Profoundly Resistant to Experimental Ischemic Stroke

Jill Roberts

University of Kentucky, jill.roberts@uky.edu

Leon de Hoog


University of Kentucky

Gregory J. Bix

University of Kentucky, gregorybix@uky.edu

Right click to open a feedback form in a new tab to let us know how this document benefits you.

Follow this and additional works at: https://uknowledge.uky.edu/sbcoa_facpub

 Part of the [Biochemical Phenomena, Metabolism, and Nutrition Commons](#), [Family, Life Course, and Society Commons](#), [Geriatrics Commons](#), [Medical Neurobiology Commons](#), and the [Neurology Commons](#)

Repository Citation

Roberts, Jill; de Hoog, Leon; and Bix, Gregory J., "Mice Deficient in Endothelial $\alpha 5$ Integrin are Profoundly Resistant to Experimental Ischemic Stroke" (2015). *Sanders-Brown Center on Aging Faculty Publications*. 84.
https://uknowledge.uky.edu/sbcoa_facpub/84

This Article is brought to you for free and open access by the Aging at UKnowledge. It has been accepted for inclusion in Sanders-Brown Center on Aging Faculty Publications by an authorized administrator of UKnowledge. For more information, please contact UKnowledge@lsv.uky.edu.

Mice Deficient in Endothelial $\alpha 5$ Integrin are Profoundly Resistant to Experimental Ischemic Stroke

Notes/Citation Information

Published in *Journal of Cerebral Blood Flow & Metabolism*, v. 37, issue 1, p. 85-96.

© Author(s) 2015

This article is distributed under the terms of the Creative Commons Attribution-NonCommercial 3.0 License (<http://www.creativecommons.org/licenses/by-nc/3.0/>) which permits non-commercial use, reproduction and distribution of the work without further permission provided the original work is attributed as specified on the SAGE and Open Access page(<https://us.sagepub.com/en-us/nam/open-access-at-sage>).


Digital Object Identifier (DOI)

<https://doi.org/10.1177/0271678X15616979>

Mice deficient in endothelial $\alpha 5$ integrin are profoundly resistant to experimental ischemic stroke

Journal of Cerebral Blood Flow & Metabolism

2017, Vol. 37(1) 85–96

© Author(s) 2015 

Reprints and permissions:

sagepub.co.uk/journalsPermissions.nav

DOI: 10.1177/0271678X15616979

jcbfm.sagepub.com

Jill Roberts^{1,2}, Leon de Hoog¹ and Gregory J Bix^{1,2,3}

Abstract

Stroke is a disease in dire need of better therapies. We have previously shown that a fragment of the extracellular matrix proteoglycan, perlecan, has beneficial effects following cerebral ischemia via the $\alpha 5\beta 1$ integrin receptor. We now report that endothelial cell selective $\alpha 5$ integrin deficient mice ($\alpha 5$ KO) are profoundly resistant to ischemic infarct after transient middle cerebral artery occlusion. Specifically, $\alpha 5$ KO mice had little to no infarct 2–3 days post-stroke, whereas controls had an increase in mean infarct volume over the same time period as expected. Functional outcome is also improved in the $\alpha 5$ KO mice compared with controls. Importantly, no differences in cerebrovascular anatomy or collateral blood flow were noted that could account for this difference in ischemic injury. Rather, we demonstrate that $\alpha 5$ KO mice have increased blood-brain barrier integrity (increased expression of claudin-5, and absent brain parenchymal IgG extravasation) after stroke compared with controls, which could explain their resistance to ischemic injury. Additionally, inhibition of $\alpha 5$ integrin in vitro leads to decreased permeability of brain endothelial cells following oxygen-glucose deprivation. Together, these findings indicate endothelial cell $\alpha 5$ integrin plays an important role in stroke outcome and blood-brain barrier integrity, suggesting that $\alpha 5$ integrin could be a novel therapeutic target for stroke.

Keywords

 $\alpha 5\beta 1$, blood-brain barrier, extracellular matrix, middle cerebral artery occlusion, transgenic

Received 7 August 2015; Revised 27 September 2015; Accepted 27 September 2015

Introduction

In ischemic stroke, a severe reduction in the blood supply to the brain leads to cell death in a region referred to as the ischemic core, and hypoxia and metabolic changes in a surrounding penumbral region that is vulnerable to injury and death over time. One strategy to treat ischemic stroke is to limit the expansion of injury and death from the initially formed core into the penumbra. Unfortunately, this experimental neuroprotective approach has stumbled in translation to human stroke patients (see Kahle and Bix¹ for a review) in no small part due to an evolving understanding of what defines the ischemic core and penumbra. Indeed, rather than being the discrete, homogeneously defined regions described above, the core and penumbra appear to be heterogeneous, each containing islands of “mini-cores” and “mini-penumbrae” with differing spatiotemporal susceptibilities to injury and death after stroke.² Understanding this complex stroke pathophysiology may be critical to developing effective therapies.

Integrins are cell surface transmembrane glycoprotein receptors for the extracellular matrix (ECM) consisting of non-covalently linked α and β subunits that, in addition to playing important roles in cell survival, proliferation, and differentiation throughout the body, play an essential role in stroke pathophysiology.^{3–5} In particular, integrins are critical to the endothelial cell-astrocyte configuration of the blood-brain barrier (BBB), whose rapid breakdown after stroke leads to edema, inflammation, and ultimately worsening stroke injury.⁶ In this context, integrins “integrate” the ECM,

¹Sanders-Brown Center on Aging, University of Kentucky, Lexington, KY, USA²Department of Anatomy and Neurobiology, University of Kentucky, Lexington, KY, USA³Department of Neurology, University of Kentucky, Lexington, KY, USA

Corresponding author:

Gregory J. Bix, University of Kentucky, Sanders-Brown Building 430, 800 S. Limestone, Lexington, KY 40536, USA.

Email: gregorybix@uky.edu

endothelial cells, and astrocyte end-feet for proper positioning and adhesion, which is disrupted after stroke.^{7–9} Under normal physiologic conditions, the BBB is made up of several layers of protection all working together to restrict the passage of substances between the blood and brain parenchyma. Tight junctions (TJ), composed predominantly of occludin, zona occludins, claudin-5, -3, and -12 and junctional adhesion molecules (JAM),¹⁰ exist between adjacent endothelial cells and are important for maintaining barrier function as they prevent paracellular transport and even restrict the passage of ions.¹¹ Disruption of integrin function not only leads to a breakdown in the BBB via ECM dysfunction but also has been recently shown to impact TJ protein expression and BBB permeability. Specifically, antibody blockade of the $\beta 1$ family of integrins (containing several different α subunit pairings) has been shown to decrease expression of claudin-5 in brain endothelial cell (BEC) monolayers in vitro and increase BBB permeability in vivo.¹² This suggests that the $\beta 1$ integrin family could play an important role in regulating BBB integrity under normal and stroke conditions. However, because integrin subunit ($\alpha 4$, $\alpha 5$, $\alpha 8$, $\beta 1$)-null mice result in embryonic lethality, the exact role of *specific* $\beta 1$ integrins in regulating BBB integrity is unknown.^{13–15}

We have previously shown that a protein fragment of the ECM proteoglycan perlecan, known as domain V (DV), is rapidly, persistently and consequently generated in the stroked brain and when systemically administered in multiple animal models of cerebral ischemia is neuroprotective and pro-angiogenic.^{16,17} This may be due, in part, to DV's interaction with its receptor $\alpha 5\beta 1$ integrin on BECs and subsequent generation and release of VEGF.^{17,18} Furthermore, DV appears to inhibit chronic post-stroke astrogliosis via interaction with astrocyte $\alpha 5\beta 1$ integrin.¹⁹ These studies, and the fact that $\alpha 5\beta 1$ integrin is conditionally upregulated in brain blood vessels after stroke,²⁰ suggest that the $\alpha 5\beta 1$ integrin, in particular, plays an important role in stroke pathophysiology.

In light of the fact that $\alpha 5$ integrin-null mice are embryonic lethal (~E10.5) due in part to defects in their vasculature,^{13–15} an endothelial-specific $\alpha 5$ integrin knockout mouse ($\alpha 5$ KO) was created to study the role of $\alpha 5$ integrin in vascular biology.²¹ This mouse, which is viable and has no obvious phenotype,²¹ exhibits significantly delayed brain angiogenesis in response to chronic cerebral hypoxia²² (8% O₂). As angiogenesis is an important component of post-stroke brain repair but is preceded by endothelial cell activation and decreased inter-endothelial cell adhesion, we here used the $\alpha 5$ KO mouse in a model of middle cerebral artery (MCA) occlusion to determine the significance of the $\alpha 5$ integrin in stroke pathophysiology and functional outcome.

Materials and methods

Animals

The experimental protocol was approved by the Institutional Animal Care and Use Committee of the University of Kentucky and experiments were performed in accordance with the Guide for the Care and Use of Laboratory Animals of the National Institutes of Health as well as the ARRIVE guidelines. All experiments were performed in a blinded fashion using randomized selection. Adult (3 months, male) mice which lack expression of the $\alpha 5$ integrin specifically in endothelial cells ($\alpha 5^{fl/-}$; Tie2-Cre; referred to here as $\alpha 5$ KO) were generated as described previously^{15,21} and generously provided by Richard Hynes (M.I.T., MA, USA). Littermate mice which do express $\alpha 5$ integrin in endothelial cells and are negative for Tie2-Cre were used as controls ($\alpha 5^{+/f}$; referred to here as Ctrl). Genotyping was performed using previously described protocols.^{15,21} All mice were housed in a climate-controlled room on a 12-h light/dark cycle and food and water were provided ad libitum.

Stroke model

Ctrl and $\alpha 5$ KO mice were subjected to transient tandem ipsilateral common carotid artery (CCA)/MCA occlusion for 60 min, followed by reperfusion of both arteries for 1–7 days. Briefly, a small burr hole was made in the skull to expose the MCA and a metal wire with a diameter of 0.005 inch was placed under the artery. Slight elevation of the metal wire causes visible occlusion of the MCA. The CCA was then isolated and occluded using an aneurysm clip. Diminished blood flow was confirmed with Laser Doppler Perfusion Monitor (Perimed, Ardmore, PA, USA) and only those animals with a diminished blood flow of at least 80% and re-establishment of at least 75% of baseline levels were included in subsequent experimentation. Animal physiologic measurements before and after stroke were made using MouseOx (Starr Life Science, Massachusetts, MA, USA). Blood was collected on post-stroke day (PSD) 3 for blood gas and ion analysis; done within 30 min after the samples were collected. To confirm stroke size and location, brains were cut into 2-mm thick coronal sections and stained with 2,3-triphenyltetrazolium chloride (TTC; BD, Sparks, MD, USA) on PSDs 1–3. Alternatively, brains were flash frozen and sectioned (20 μ m) to undergo cresyl violet (Sigma) staining. Infarct size was analyzed using Image J (NIH) and infarct volume was calculated as,

$$\text{Infarct Volume} = \text{Apparent Infarct} \\ - (\text{Contralateral Hemisphere/Ipsilateral Hemisphere})$$

Animals were excluded from the study if the middle cerebral or CCA was punctured during wire and clamp insertion or removal, died following surgery in recovery or were euthanized before the end of the study due to poor health. Overall, there is <5% death rate for our stroke model both following surgery and during behavioral testing.

Behavioral testing

Animals were tested on the Rotor Rod to examine forced motor coordination. Behavioral testing took place for 3 days prior to stroke surgery (training and baseline measurement) and on PSDs 1 and 7. The mice were placed on the Rotor Rod for 5 min with an increasing acceleration from 0 to 40 rpm for three trials and the parameters were set to measure latency in seconds.

Vessel staining and vascular territory

Cerebrovascular anatomy of the $\alpha 5$ KO and Ctrl mice was measured by intravenous injection of a combination of two carbon ink dyes as previously described.²³ Briefly, papaverine hydrochloride (50 mg/kg; Sigma, St. Louis, MO, USA) was injected intravenously for vessel dilation just prior to the injection of carbon ink. A mixture of ink 1 (Fount India, Pelikan, Germany) and ink 2 (Super Black, Speedball, USA) was intravenously injected at a ratio of 1:9, respectively. After 10 min, the brain was removed and fixed in 4% paraformaldehyde prior to images being taken with a Moticam 2 (Motic, British Columbia, Canada) camera and software. Points of anastomoses between the MCA and the anterior cerebral artery (ACA) were determined and the total area of the MCA and ACA was measured using Image J software (NIH).

Blood perfusion imaging

Cortical blood flow was monitored using a blood perfusion imager (PeriCam PSI System, Perimed) based on Laser Speckle Contrast Analysis technology. Briefly, the skin was retracted to expose the skull of the animal and the imager was positioned above the head. The laser detects movement in tissue, such as red blood cells, and creates speckle contrast. Measurement in the contrast fluctuations provides information about blood perfusion in the brain. Baseline (5 min) measurements of blood flow were first obtained and the animal was then subjected to the stroke model. Immediately following occlusion of the CCA/MCA, blood flow measurements were taken for another 5 min. Measurements were also recorded following reperfusion of the CCA/MCA, confirming the re-establishment of blood flow. Only animals with at least a 30% decrease in total blood perfusion following occlusion were included in subsequent analysis. Regions of interest equal in size

(encompassing the visible region of the MCA) were used to determine the perfusion in the ipsilateral and contralateral hemispheres of the Ctrl and $\alpha 5$ KO mice. Blood perfusion is expressed in arbitrary units (Perfusion Units).

Tissue histology and immunohistochemistry

On PSDs 1–3, brains were removed, flash frozen and stored at -80°C until use. Brains were cut into 20- μm sections using a cryostat and mounted onto slides. Sections were fixed with ice cold acetone prior to incubating in blocking buffer (5% BSA in phosphate buffered saline (PBS) with 0.1% Triton X-100) for 1 h at room temperature. The sections were then incubated overnight at 4°C in the primary antibody against IgG (1:1000; Life Technologies). Sections were washed and incubated with a secondary antibody (HRP anti-mouse, Life Technologies) for 1 h at room temperature. Sections were washed and incubated with DAB (Vector Labs, Burlingame, CA, USA) for 1 h prior to counterstaining with hematoxylin (Fisher Scientific, USA). Alternatively, sections were stained with primary antibodies against fluorescein isothiocyanate (FITC)-conjugated-tomato lectin (1:200; Vector Labs), glial fibrillary acidic protein (GFAP) (1:500, Sigma), terminal deoxynucleotidyl transferase dUTP nick end labeling (TUNEL) (Apoptag Fluorescien kit, Millipore), or cresyl violet (Sigma) overnight at 4°C . Slides were then coverslipped with fluorescent mounting media (Vector Labs) or xylene-based mounting media (Sigma) and images were captured using a Nikon Eclipse Ti microscope and software (Nikon, Melville, NY, USA).

Gene expression

On PSDs 1–3, brains were removed and cut into 2-mm thick sections. The sections were cut to separate the two hemispheres and the ipsilateral hemisphere was trimmed to remove striatum (leaving cortical ischemic core and penumbra). All ipsilateral sections/animal were combined, and tissue was homogenized in Trizol (Life Technologies). RNA was extracted according to the instructions of the RNA extraction kit manufacturer (Life Technologies). RNA was converted to cDNA using a high capacity cDNA reverse transcription kit (Applied Bioscience, Grand Island, NY, USA). Claudin-5 and 18S (control) genes were analyzed using Real-time PCR (ViiA7; Life Technologies). Data were analyzed comparing $\alpha 5$ KO to Ctrl mice and are presented as a % of control (sham mice).

Oxygen-glucose deprivation (OGD)

Stroke was modeled in vitro via OGD. C57/Bl6 mouse BECs¹⁷ (immortalized; Ctrl) were plated and once confluent incubated in either glucose-depleted Dulbecco's

Modified Eagle Medium supplemented with 1% FBS, 1× antibiotic/antimycotic and 1% L-glutamine (Life Technologies) or control medium which contained 4.5 g/l glucose Dulbecco's Modified Eagle Medium identically supplemented with the aforementioned compounds. Cells undergoing OGD were then placed in a Modular Incubator Chamber (Billups-Rothenberg Inc., CA, USA) and flushed with N₂ for 5 min to displace O₂ levels, whereas the control plate (normoxic conditions) was not flushed with N₂, but left in O₂ for 5 min. Subsequently, the chamber was moved to an incubator at 37°C and 5% CO₂ for 8 h. The control plate was placed in the same incubator. At the end of the OGD period, cells were re-oxygenated and re-gluconated for 24 h by exchanging the glucose-depleted medium (or control medium) back for the normal cell medium and placed into the incubator.

Permeability assays

BECs (as above) were plated on Transwell Permeable plates (Corning, Tewksbury, MA, USA) at a density of 50,000 cells/insert and incubated at 37°C until a confluent monolayer formed. Cells were then exposed to OGD for 8 h and allowed to re-oxygenate/re-gluconate for 24 h. Following 4 h of re-oxygenation, cells were treated with the small peptide $\alpha 5\beta 1$ integrin inhibitor ATN-161 (10 μ M, MedKoo Biosciences, Chapel Hill, NC) or vehicle for the remaining re-oxygenation period. Inserts were then treated with FITC-dextran (4 kDa, 10 μ g/ml, Sigma-Aldrich, St. Louis, MO) and incubated at 37°C for 60 min. Samples (200 μ l) from the wells were collected at 30 and 60 min and transferred to a 96-well plate. The volume collected from the well was replaced with an equal volume of cell medium. Subsequently, a fluorescent plate reader was used to measure fluorescence of these samples at 528 nm. Here, increased fluorescence indicates an increase in permeability. Additionally, permeability was indirectly determined by measuring trans-endothelial electrical resistance (TEER) across the cell monolayer using an Epithelial Voltmeter (World Precision Instruments, Sarasota, FL, USA). Here, decreased resistance indicates an increase in permeability.

Statistical analysis

Experiments were conducted in accordance to the STAIR recommendations²⁴ and, where applicable, were performed in a blinded and randomized fashion. All measured variables are presented as mean \pm SEM from a minimum of three independent experiments. We conducted a power analysis to ensure adequate subject numbers as detailed in the figure legends for each study. Analysis of results for comparison between Ctrl and $\alpha 5$ KO groups was performed using a Student's *t*-test. For

time course comparisons, a two-way repeated measures analysis of variance (ANOVA) was used. Significance is defined as a **p* \leq 0.05, ***p* \leq 0.01, and ****p* \leq 0.001.

Results

$\alpha 5$ KO mice have smaller infarct volumes following stroke

Ctrl and $\alpha 5$ KO mice underwent tandem transient ipsilateral CCA/MCA occlusion surgery with reperfusion of 1–3 days. On PSDs 1, 2, or 3, brains were analyzed using TTC stain and the volume of white, TTC negative area in the cortex was measured (Figure 1(a) and (b)). As expected, the infarct volume in the Ctrl animals increased with time, reaching the peak infarct volume by PSDs 2–3.¹⁷ While the infarct volume in $\alpha 5$ KO animals appeared to be small and of similar size to the Ctrl on PSD 1, to our surprise, the infarct remained similarly sized on PSD 2 and was virtually non-detectable on PSD 3. A significant (*p* < 0.05) difference between the Ctrl and the $\alpha 5$ KO animals is observed on PSD 2 (37.9 \pm 2.6 vs. 5.2 \pm 1.3 mm³, respectively) and PSD 3 (38.3 \pm 2.6 vs. 0.1 \pm 0.6 mm³, respectively) (Figure 1(b)). Of note, no significant differences in vital signs (heart rate, temperature) immediately before or after stroke were noted, nor were there any significant differences in pre-stroke or PSD body weight (data not shown). General physiological parameters (blood gas analysis) were also not different between Ctrl and $\alpha 5$ KO animals (data not shown).

$\alpha 5$ KO animals have better post-stroke function

To determine whether functional differences exist between Ctrl and $\alpha 5$ KO animals after stroke, forced motor coordination was studied using a Rotor Rod. Baseline measurements were obtained prior to MCA/CCA occlusion model (no significant differences were noted in raw baseline performance on the rotor rod between the two groups) and the animals were again tested on PSDs 1 and 7. By PSD 7, the $\alpha 5$ KO animals had shown a significant (*p* < 0.01) improvement over their own baseline levels (152.4 \pm 10.9 vs. 100.0 \pm 6.7% baseline, respectively), but more importantly had a significantly (*p* < 0.05) longer latency on the Rotor Rod when compared with the Ctrl (152.4 \pm 10.9 vs. 114.5 \pm 10.4% baseline, respectively), but not when compared with naïve animals (data not shown), at PSD 7 (Figure 1(c)), indicating better post-stroke functional outcome with a return to standard levels.

Cerebral vasculature does not appear different between Ctrl and $\alpha 5$ KOs

We next used several approaches to determine whether alterations in cerebral vasculature between Ctrl and

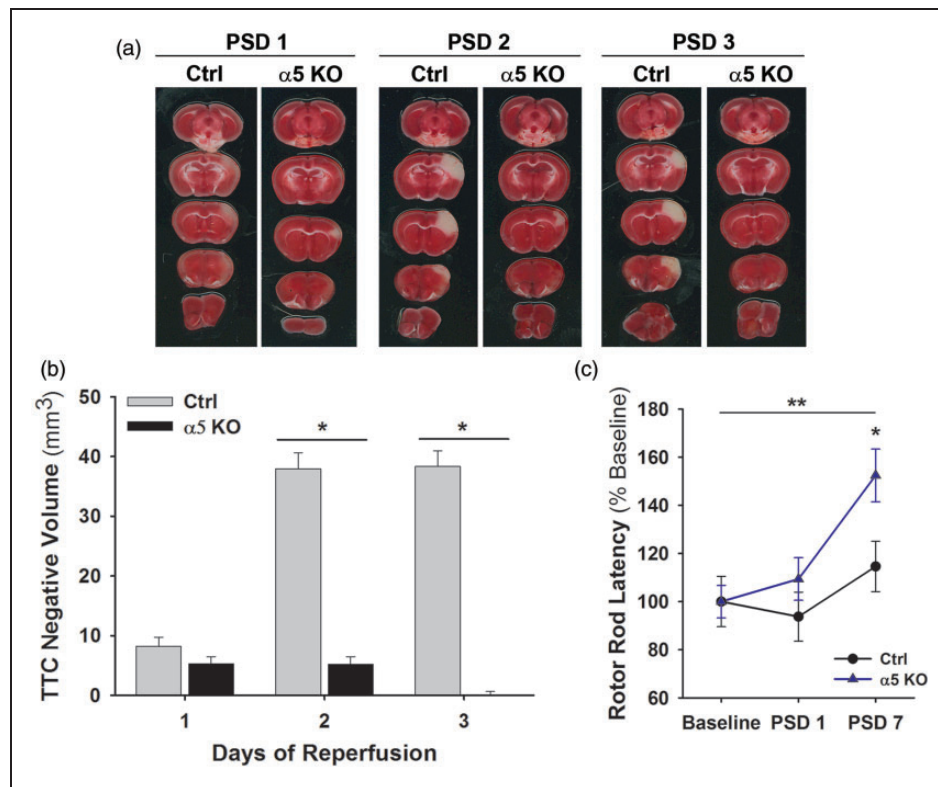


Figure 1. Infarct volume in $\alpha 5$ KO mice is significantly smaller than Ctrl mice following transient MCA occlusion. (a) Representative images of Ctrl and $\alpha 5$ KO brain sections stained with TTC on PSDs 1–3. (b) Quantification of TTC negative (white) area in sections from Ctrl and $\alpha 5$ KO mice on PSDs 1–3. * $p < 0.05$ compared to Ctrl animals at same time point. $N = 12$. (c) $\alpha 5$ KO animals have improved functional behavior compared to Ctrl mice. Graph shows latency (% of baseline) on Rotor Rod functional test prior to stroke and on PSDs 1 and 7. The $\alpha 5$ KO animals have a significant improvement in latency compared to the Ctrl animals. * $p < 0.05$ compared to Ctrl at same time point and ** $p < 0.01$ compared to $\alpha 5$ KO baseline values. $N = 6$. MCA: middle cerebral artery; TTC: triphenyltetrazolium chloride; PSD: post-stroke day.

$\alpha 5$ KO mice could contribute to the differences we observed in the infarct volumes. First, we observed blood vessels in the brain tissue via tomato lectin (T-Lectin) immunohistochemistry and found no significant difference in cerebrovascular density between the groups (100.0 ± 3.8 vs. $92.8 \pm 6.5\%$ Ctrl) (Figure 2(a)). We then examined the architecture and cerebrovascular territory of the MCA and ACA. Following injection of the blood vessel dilator, papaverine, we intravenously injected carbon black ink to visualize the cerebral blood vessels.²³ Figure 2(b) shows the territory of the MCA (shaded pink) and when quantified demonstrates that there is no significant difference in the MCA territory area between the Ctrl and $\alpha 5$ KO (21.5 ± 0.8 vs. 19.9 ± 0.7 mm², respectively) animals. There was also no difference in the territory area of the ACA (data not shown). Therefore, no differences in brain blood vessel density or cerebrovascular anatomy exist that could otherwise explain the differences observed in infarct volume between the Ctrl and $\alpha 5$ KO animals.

Likewise, to determine whether potential differences in collateral blood flow to the MCA brain territory

could exist between the Ctrl and $\alpha 5$ KO mice, which might also explain the infarct volume differences, we observed cortical blood flow in real time using a PeriCam PSI System imager. This system measures the movement of red blood cells in the cortex using a speckle laser, providing information about blood perfusion over time. Baseline measurements were recorded over a 5-min period prior to subjecting the animals to the MCA/CCA occlusion model. Immediately following vessel occlusion, perfusion measurements were recorded for another 5-min period. After 60 min of occlusion, the animals were re-perfused. Figure 2(c) shows representative images of cortical perfusion in Ctrl and $\alpha 5$ KO animals. A significant ($p < 0.05$) decrease in blood flow within the ipsilateral hemisphere is observed following MCA/CCA occlusion in both Ctrl (33.99% decrease from baseline) and $\alpha 5$ KO (33.97% decrease from baseline) animals (Figure 2(c)). Although blood perfusion is slightly higher in the $\alpha 5$ KO mice, it is important to note that no significant difference in overall perfusion (baseline levels, post-occlusion levels, or reperfusion levels) is observed

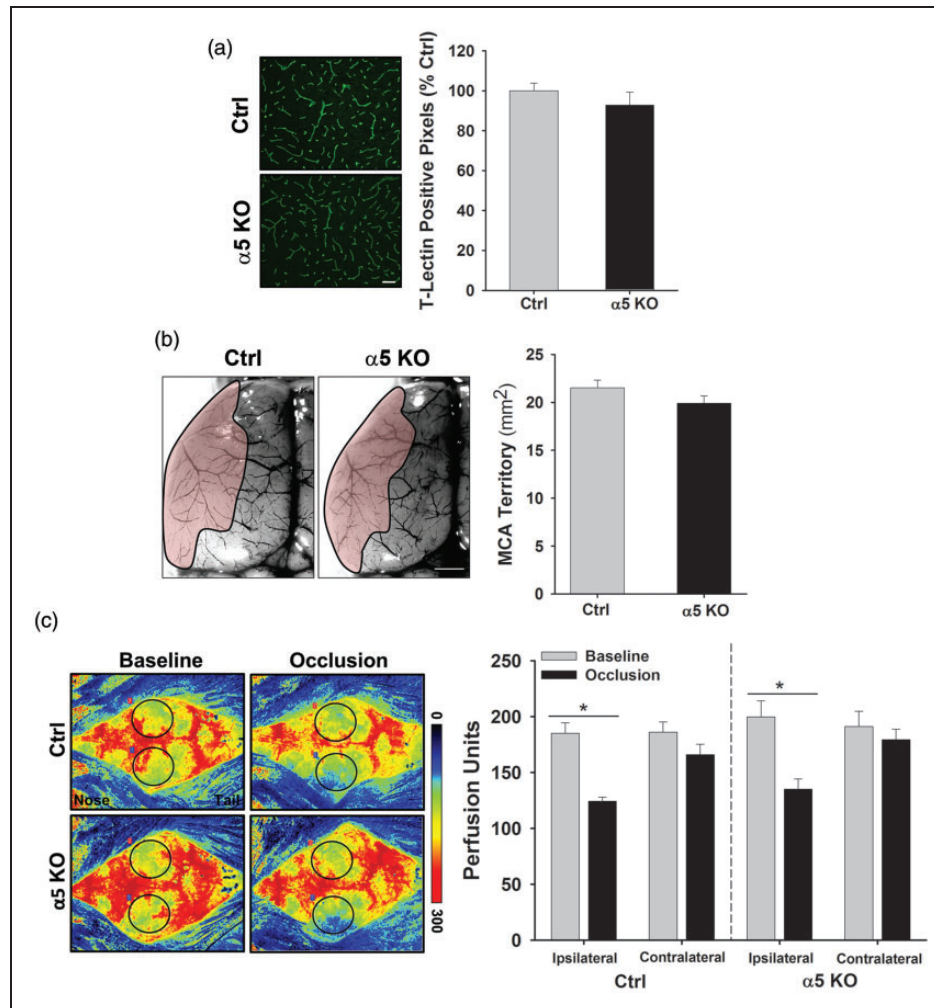


Figure 2. Cerebral vasculature is similar between Ctrl and $\alpha 5$ KO animals. (a) Representative images of cortical brain sections immunostained with T-Lectin to visualize endothelial cells/blood vessels in Ctrl and $\alpha 5$ KO animals. Graph is quantification of T-Lectin positive pixels and indicates no significant difference between the groups. Scale bar = 50 μ m. N = 3. (b) Representative images of brains (left hemisphere) injected with carbon black ink to visualize the blood vessels. MCA territory (shaded pink) was determined by finding anastomoses points between the MCA and ACA and then outlining MCA region. Graph shows quantification of MCA area, with no significant difference between groups. Scale bar = 1 mm. N = 9. (c) Representative images of Laser Speckle analysis of blood perfusion in Ctrl and $\alpha 5$ KO animals. Baseline and occlusion images show areas of red as high blood perfusion and areas of blue as low blood perfusion. Graph indicates quantification of blood perfusion in MCA regions of interest (black circle) in ipsilateral and contralateral hemispheres. A significant decrease is observed following occlusion in the ipsilateral hemisphere, but no difference is observed between Ctrl and $\alpha 5$ KO animals. * $p < 0.5$ compared to baseline measurements. N = 6. MCA: middle cerebral artery; ACA: anterior cerebral artery.

between the two groups. This suggests that there is no significant difference in collateral flow, which would contribute to the differences observed in infarct volume.

$\alpha 5$ KO mice have less neuronal pathology and cell death following stroke

To better visualize potential differences in brain histopathology between stroked Ctrl and $\alpha 5$ KO mice, we examined cresyl violet-stained brain sections from these animals on PSDs 1 and 3 (Figure 3(a)). On PSD 1,

where similar volume “infarcts” were identified by TTC stain, neurons appear small, pyknotic, and less dense in the Ctrl brains compared with the $\alpha 5$ KO brains. In fact, neurons of the ipsilateral hemisphere in the $\alpha 5$ KO animals look very similar to the neurons of the contralateral hemisphere, indicating little to no change in morphology following stroke. Interestingly, there is little to no apoptotic cell death in the tissue of $\alpha 5$ KOs on PSD 1 (378.5 ± 99.5 pixels) or PSD 3 (297.1 ± 121.2 pixels) compared with Ctrl animals (PSD 1, 6010 ± 1829 pixels; PSD 3, $25,053 \pm 1653$

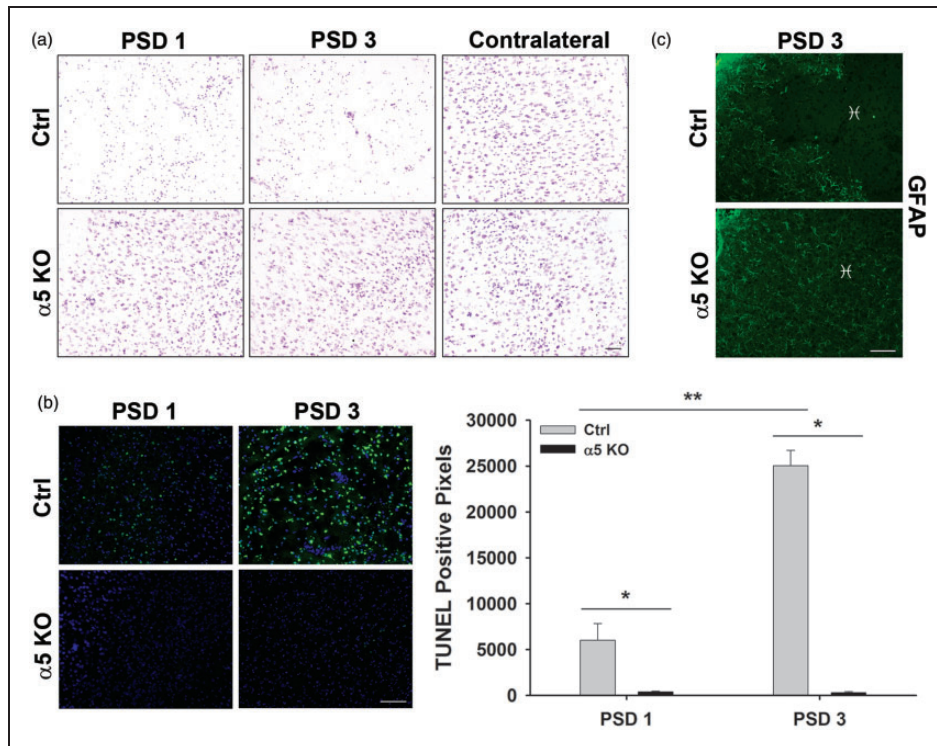


Figure 3. Significantly less cell death occurs in the $\alpha 5$ KO animals compared with theCtrls. (a) Representative images of cresyl violet staining in cortical regions of brains from Ctrl and $\alpha 5$ KO animals following stroke. Neurons within infarct region of Ctrl mice are small, pyknotic, and fewer in number compared with $\alpha 5$ KOs, which appear to have normal looking neurons, when compared with the contralateral hemisphere. Scale bar = 50 μ m. N = 6. (b) TUNEL (green) staining of infarct region on PSDs 1 and 3 and quantification of TUNEL-positive pixel staining indicate an increase in cell death overtime in the Ctrl animals with very little cell death observed in the $\alpha 5$ KOs. DAPI (blue) counterstain. Scale bar = 50 μ m. * $p < 0.05$, ** $p < 0.01$, N = 6. (c) GFAP staining of infarct region (X) on PSD 3 shows lack of astrocytes in infarct core of Ctrl tissue and normal distribution of astrocytes in $\alpha 5$ KO tissue. Scale bar = 50 μ m. N = 3. PSD: post-stroke day.

pixels), as observed by TUNEL staining (Figure 3(b)). Taken together, $\alpha 5$ KO animals appear to be protected against cell death following a stroke, unlike the Ctrl animals.

To examine whether the activation of astrocytes plays a role in the infarct size differences observed between these animals, we performed immunohistochemistry for GFAP. On PSD 3, Ctrl animals show an apparent lack of GFAP staining in the infarct core region (Figure 3(c)), while tissue surrounding the core maintains a normal (non-activated) expression level. In comparison, the $\alpha 5$ KO animals have an even distribution of GFAP staining throughout the cortex, including the “infarcted” region (Figure 3(c)). Therefore, while there are differences in GFAP expression between WT and $\alpha 5$ KO mice, there does not appear to be an increase in *activated* astrocytes at this time point, suggesting the differences in infarct volume between these mice is not due to astrocyte activation and subsequent reduction in TTC negative staining.

Changes in BBB function

The ECM and its integrin receptors contribute to the integrity of the BBB. After stroke, disruption/degradation of the ECM and alteration of its interaction with integrins contributes to the breakdown of the BBB and subsequent edema, inflammatory cell infiltration, and neuronal death. This cascade of events is a major contributor to the expansion of ischemic injury and cell death that occurs over time after stroke. As our results suggest that ischemic injury is minimal and does not expand over time in $\alpha 5$ KO mice, we hypothesized that this could be due to differences in BBB integrity in these mice after stroke. To test this hypothesis, we performed IgG immunohistochemistry on brain sections from Ctrl and $\alpha 5$ KO animals on PSDs 1–3. IgG (approximately 150 kDa) will penetrate brain parenchyma only if the BBB is disrupted. We were unable to detect *any* IgG in the brain parenchyma of the $\alpha 5$ KO mice at any PSD, while it was abundant in the Ctrl brains at PSDs 1–3 (Figure 4(a)). This suggests that the BBB remains relatively intact in

the $\alpha 5$ KO mice after stroke compared with Ctrl animals.

Next, as pan- $\beta 1$ integrin inhibition has been directly linked to decreased TJ protein claudin-5 expression and decreased BBB integrity,¹² we hypothesized that endothelial cell selective KO of $\alpha 5(\beta 1)$ integrin could increase BBB integrity by affecting post-stroke TJ protein expression. Using real-time PCR, we examined the TJ protein claudin-5 after stroke and determined that while baseline claudin-5 gene expression levels are similar in sham animals between Ctrl and $\alpha 5$ KO mice, stroke causes a significantly smaller drop in claudin-5 gene expression in $\alpha 5$ KO mice on PSD 1 compared with Ctrl levels (0.81 ± 0.03 vs. 0.52 ± 0.08 fold, respectively) (Figure 4(b)). These data suggest that $\alpha 5$ KO mice have differently regulated BBB components after

stroke that may contribute to its increased post-stroke integrity.

Inhibition of $\alpha 5$ integrin maintains barrier integrity in vitro after OGD

To further investigate the effects of $\alpha 5$ integrin on brain endothelial barrier function, we examined in vitro BEC monolayer permeability using a small peptide inhibitor of $\alpha 5\beta 1$ integrin, ATN-161.²⁵ Employing a TEER assay (an indirect measure of cell monolayer permeability where greater TEER is indicative of lower permeability, etc.), we found that BECs treated with ATN-161 under normoxic conditions had similar TEER values as PBS vehicle (Ctrl) treated cells (Figure 5(a)). However, following OGD (8 h) and 24 h of re-oxygenation to mimic

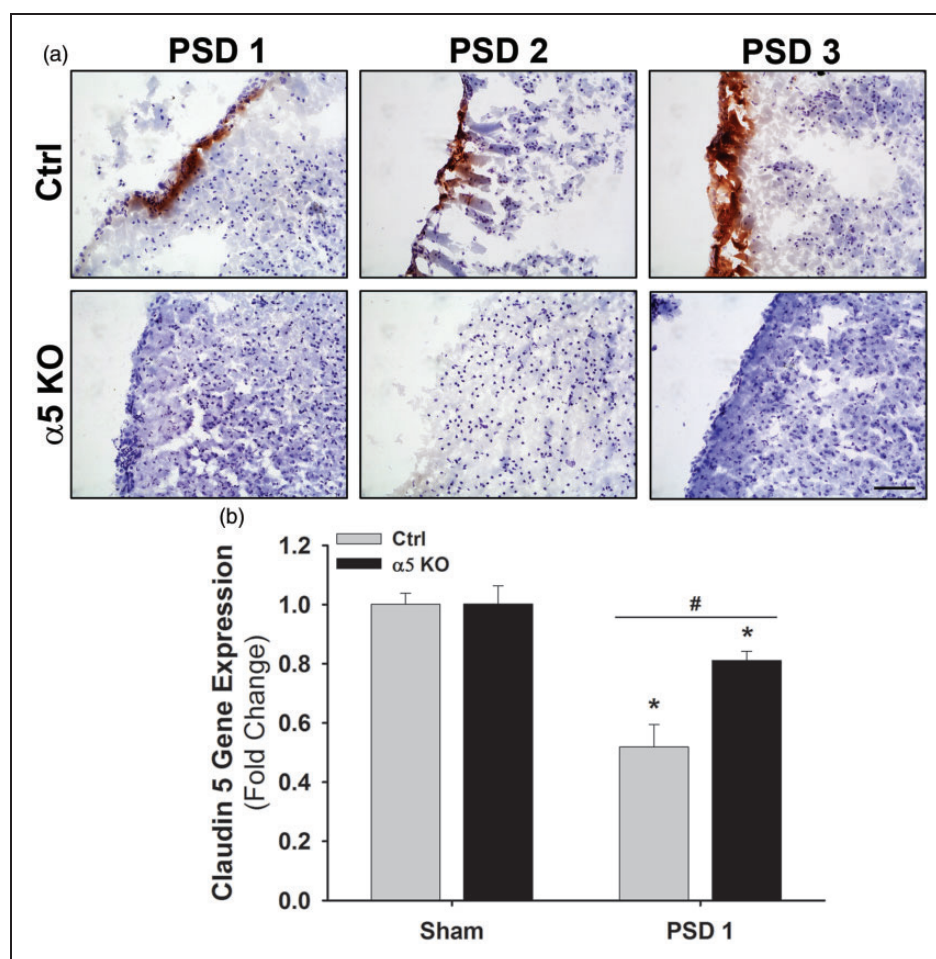


Figure 4. BBB integrity is preserved in $\alpha 5$ KO animals compared with Ctrl animals following cerebral ischemia. (a) Representative images of brain tissue (infarcted region) stained for IgG (brown) and counterstained with hematoxylin (purple) in Ctrl and $\alpha 5$ KO animals on PSDs 1–3. Scale bar = 50 μ m. N = 3. (b) Gene expression of Claudin 5 in Ctrl and $\alpha 5$ KO tissue (ipsilateral hemisphere) following cerebral ischemia. A significant decrease is observed on PSD 1, but the decrease in $\alpha 5$ KO tissue is not as great as in Ctrl. * $p < 0.05$ compared to Ctrl sham and # $p < 0.05$ compared to Ctrl animals at same time point. N = 3. BBB: blood-brain barrier; PSD: post-stroke day.

the ischemia/reperfusion of stroke, Ctrl cells, but *not* ATN-161-treated cells, had significantly reduced TEER (greater permeability) compared with normoxic conditions (Figure 5(a)). Next, BEC monolayer permeability was directly measured with FITC-dextran (Figure 5(b)). Under normoxic conditions, the ATN-161-treated BECs showed lower levels of fluorescence (lower permeability) compared with Ctrl BECs. Following OGD, Ctrl cells significantly increased their permeability while cells treated with ATN-161 maintained levels consistent with normoxic conditions (Figure 5(b)). Taken together, blockade of $\alpha 5$ integrin on endothelial cells helps maintain a tighter barrier under both normoxic and OGD conditions.

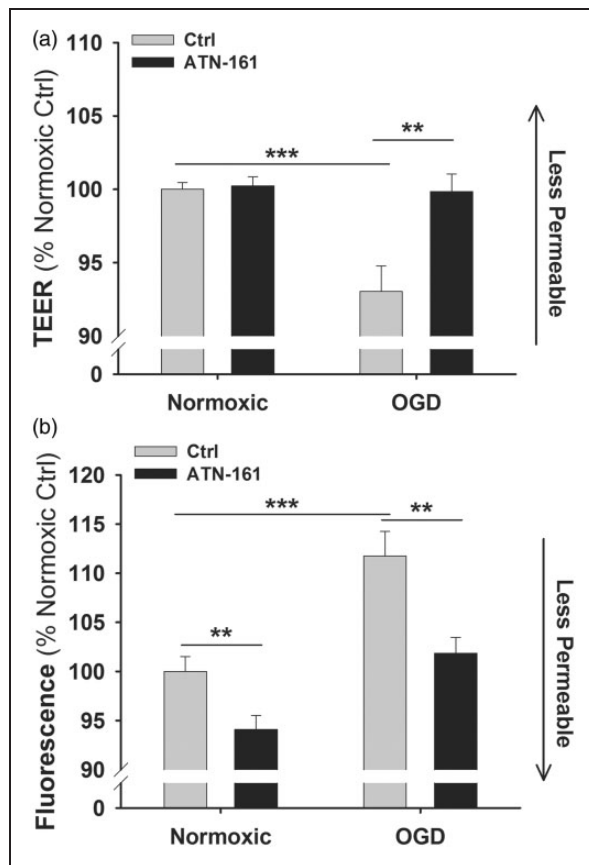


Figure 5. $\alpha 5$ integrin inhibition maintains barrier integrity. (a) TEER permeability assay of PBS vehicle-treated (Ctrl) and ATN-161-treated endothelial cells under normoxic or OGD conditions. Graph presented in % change from Ctrl normoxic conditions. ** $p < 0.01$ and *** $p < 0.001$ compared to Ctrl. $N = 3$. (b) FITC-dextran permeability assay of Ctrl and ATN-161-treated endothelial cells under normoxic or OGD conditions. Graph presented in % change from Ctrl normoxic conditions. ** $p < 0.01$ and *** $p < 0.001$ compared to Ctrl. $N = 3$. TEER: trans-endothelial electrical resistance; OGD: oxygen-glucose deprivation.

Discussion

In this study, we demonstrate that mice with an endothelial cell selective deletion of $\alpha 5$ integrin have profoundly smaller infarcts and functional deficit after transient MCA/CCA occlusion. Importantly, this apparent resistance to ischemic injury cannot be explained by differences in vital statistics, blood gas, serum electrolytes, cerebral vasculature (macrovasculature on the brain surface or smaller blood vessels within the brain parenchyma in agreement with the angiogenic and vasculogenic analysis in the original report of these animals²¹) blood flow, or infiltration or activation of GFAP cells into the stroke affected area, as none of these variables significantly differ between Ctrl and $\alpha 5$ KO mice. Rather, our results suggest that $\alpha 5$ KO mice resist ischemic stroke injury due to greater post-stroke BBB integrity, resulting in less BBB leakage and resultant expansion of ischemic injury. This is demonstrated by absent IgG extravasation into the brain parenchyma in $\alpha 5$ KO mice after stroke, relatively increased levels of the TJ protein claudin-5 compared with Ctrl, as well as decreased permeability in cells treated with the $\alpha 5\beta 1$ integrin inhibitor ATN-161 under both normoxic and OGD (stroke-like) conditions. To the best of our knowledge, this is the first study to link endothelial cell $\alpha 5\beta 1$ integrin to resistance to ischemic injury via increased BBB integrity.

The importance of the BBB for maintaining the homeostasis of the brain is well known. Cerebrovascular permeability is controlled by the endothelial cells and their TJs, proteins, and integrins of the ECM, as well as pericytes and astrocytes. During ischemia, permeability of the BBB increases due to dysfunction, disassembly (e.g. of TJ proteins), and differential regulation (e.g. decreases in TJ expression and increases in ECM-processing proteases) in one or all of these factors. As described by Sandoval and Witt,²⁶ three phases of paracellular permeability may occur following post-stroke reperfusion; an initial reperfusion permeability associated with re-establishment of blood flow, and a “bi-phasic” response, which may occur hours to days following injury. This increase in permeability may contribute to the continuously evolving infarct, which may occur over a period of days depending on the form of animal stroke model used for assessment. For example, we show here, as well as in our previous work¹⁷ and the work of others^{27,28} that the size of the infarct gradually increases in size following transient MCA/CCA occlusion, becoming maximal by PSD 3. In contrast, $\alpha 5$ KO mice in this stroke model show limited early injury (TTC-negative area) that both fails to expand and appears to rapidly regress, possibly due to a tightening of the BBB and a decrease in the number of phasic events. Importantly, while TTC analysis suggests that the size of the infarct between Ctrl

and $\alpha 5$ KO mice appears to be similar on PSD 1, our cresyl violet and TUNEL stain analysis (Figure 3) demonstrates that the TTC-negative area on PSD 1 in the $\alpha 5$ KO mice actually contains few pyknotic and apoptotic cells, which persists out to PSD 3. These seemingly discrepant results may be due to the fact that while TTC staining is traditionally used as a measure of stroke infarct area, i.e. dead cells, it is *actually* a measurement of mitochondrial functional activity. Likewise, we did not detect any significant increase in other cell types, such as GFAP-positive astrocytes, into the ipsilateral brain on PSDs 1–3 that could restore TTC-positive signal to this area and thereby otherwise explain this result. Therefore, we conclude that this TTC-negative area contains stressed, but surviving cells which produce an insufficient level of formazan (TTC stain) to be detected macroscopically on PSD 1,²⁹ but, in the absence of continued insult secondary to a more stable BBB, gradually recover and are again TTC positive. In fact, the ischemic core and penumbra is a heterogeneous region, with pockets of both dead and live cells.² Therefore, the permeability of the BBB over time may play a large role in the survival of injured tissue following stroke, particularly so in our transient stroke model with a slowly evolving infarct. For this reason, studies employing stroke models with a more rapidly evolving infarct size, including permanent occlusion models, should shed further light on the nature of $\alpha 5$ KO mice resistance to ischemic injury. Likewise, serial imaging experiments (ongoing in our lab) are necessary to further evaluate the temporal nature of the infarct (or lack thereof) within each individual stroked $\alpha 5$ KO mouse.

A potential link between the $\beta 1$ family of integrins and BBB permeability has recently been suggested.¹² In these studies, treatment with the pan- $\beta 1$ integrin function blocking antibody Ha2/5 increased primary BEC monolayer permeability in vitro while simultaneously decreasing their claudin-5 expression at the cell surface. Likewise, in vivo stereotactic injection of Ha2/5 into the striatum of mice resulted in increased IgG extravasation into the brain parenchyma as compared with stereotactically injected IgM control. However, the use of a pan- $\beta 1$ integrin functioning blocking antibody in these studies by design made it impossible to determine the relative contribution of any particular $\alpha(x)\beta 1$ integrin to this BBB permeability effect. Furthermore, the potential for this antibody to interact with and block the function of $\beta 1$ integrin expressed on additional cell types in addition to endothelial cells when stereotactically injected into the brain striatum, and thereby also impact BBB permeability, could not be completely ruled out. For these reasons, we chose to focus on a specific $\beta 1$ integrin whose deletion was limited to endothelial cells.

Of the various $\beta 1$ integrin receptors known to be expressed in BECs, we chose to focus on $\alpha 5\beta 1$ for a number of reasons. Although highly expressed in brain microvasculature during development, $\alpha 5\beta 1$ integrin is virtually absent in these cells in the mature brain. However, $\alpha 5\beta 1$ integrin expression is significantly upregulated in BECs following global hypoxia or ischemic stroke^{22,30} (in peri-infarct regions). In both cases, it has been shown to have an important role in post-injury angiogenesis²² and endothelial cell selective $\alpha 5$ KO mice (the same as used in our study) have a significantly delayed brain angiogenic response following global cerebral hypoxia.²² Additionally, we have identified $\alpha 5\beta 1$ integrin as a key receptor for the beneficial angiogenic effects of perlecan domain V in treating experimental ischemic stroke.¹⁷ Therefore, deletion of $\alpha 5$ integrin on endothelial cells would be predicted to have a negative impact on angiogenesis following cerebral ischemia, leading to deficient post-stroke neurorepair and worse functional outcomes. Indeed, it was our expectation to demonstrate this when we initially subjected the $\alpha 5$ KO mice to MCA occlusion rather than to discover any potential effects on the extent of ischemic injury in these mice. However, endothelial cell activation and associated ECM proteolysis (via MMP2 and other proteases) that occurs after ischemic stroke and as an early stage of angiogenesis all contribute to increased BBB permeability. Therefore, it stands to reason that if post-stroke endothelial cell upregulation of $\alpha 5\beta 1$ integrin is a component of this endothelial cell activation, ECM proteolysis and subsequent angiogenesis, it also has the potential to significantly contribute to the resultant decreased integrity of the BBB and expansion of injury that occurs. In this light, our results support the novel conclusion that BEC $\alpha 5\beta 1$ integrin upregulation after ischemic stroke is a component of endothelial cell activation that directly contributes to post-stroke breakdown of the BBB and resultant worsening of ischemic injury. Here, we report that inhibition of $\alpha 5\beta 1$ on BECs show decreased permeability under OGD conditions compared with Ctrl cells. These results were also observed under normoxic conditions when measured by FITC-dextran (4 kDa) versus TEER. Discrepancies in the normoxic condition between these methods may possibly be due to differences in detection sensitivity. Ultimately, these results indicate that inhibition of $\alpha 5$ integrin on endothelial cells lead to a tighter barrier in vitro. In the $\alpha 5$ KO mouse, BECs may be resistant to activation after stroke as a result of their inability to upregulate $\alpha 5\beta 1$ integrin, resulting in less of a decrease in claudin-5, contributing to or resulting in retained BBB integrity and ultimately minimal ischemic injury. Likewise, the delayed, but ultimately not absent brain angiogenesis that was observed by Li et al.²² in the $\alpha 5$ KO mice after

continuous exposure to global hypoxia might indicate a similar resistance to hypoxia-induced endothelial cell activation that is only gradually overcome by the continually present (over several days) hypoxic conditions. Ultimately, a variety of BBB components (other TJ proteins, markers of permeability, etc.) must be examined to better understand the link between $\alpha 5\beta 1$ integrin and BBB integrity.

Our results with the $\alpha 5$ KO mouse suggest that brain endothelial $\alpha 5\beta 1$ integrin could represent a novel therapeutic target in the acute or subacute phase after ischemic stroke. However, the timing of such a therapy (i.e. to stabilize the BBB and minimize injury in the short term without impeding more chronic angiogenic neurorepair) as well as the ability to selectively target endothelial cells may represent challenges to such a treatment strategy. Indeed, in our own previous work, intravenous treatment with $\alpha 5\beta 1$ integrin function blocking antibody on PSDs 1–3 after transient MCA occlusion in wild-type mice resulted in slightly (but significantly) larger ischemic infarcts on PSDs 2 and 3 and diminished peri-infarct angiogenesis on PSDs 5–7.¹⁷ This seemingly contradictory effect of $\alpha 5\beta 1$ integrin blockade on ischemic infarct size is likely due to the experimental design used in the previous study—a systemic route of administration in combination with an antibody inhibitor that would non-cell selectively bind to and inhibit the $\alpha 5\beta 1$ integrin wherever it encountered it throughout the body (i.e. not limited to endothelial cells), an especially important consideration as $\alpha 5\beta 1$ is expressed in many different cell types throughout the body such as platelets and chondrocytes.^{31,32} In support of this conclusion, preliminary studies in our lab with systemic administration of ATN-161, a peptide $\alpha 5\beta 1$ integrin inhibitor that specifically targets and inhibits *activated* $\alpha 5\beta 1$ (i.e. not the vast majority of quiescent $\alpha 5\beta 1$ integrin throughout the body) integrin^{25,33} 24 h after MCA occlusion in Ctrl mice mimics the results of diminished ischemic injury seen in the $\alpha 5$ KO mouse in this report. This suggests that selective targeting of activated $\alpha 5\beta 1$ integrin as occurs in peri-infarct vasculature may be a valid therapeutic approach for stroke worthy of further investigation.

In conclusion, we report for the first time that mice with selective endothelial cell knockout of $\alpha 5$ integrin are resistant to stroke injury. The lack of infarct observed by PSD 3 may be due to maintenance of the BBB integrity, unlike the Ctrl animals, which experience increased BBB permeability. It is possible that the absence of $\alpha 5$ integrin decreases the number of BBB phasic opening events, therefore decreasing the potential for secondary injury by infiltrating cells and molecules, limiting injury and affording rapid recovery. Further studies will expand our knowledge of the role this integrin plays in BBB integrity and its potential as a novel stroke therapeutic target.

Funding

The author(s) disclosed receipt of the following financial support for the research, authorship, and/or publication of this article: NIH 2R01NS065842-08 to G.J.B.

Acknowledgments

We would like to acknowledge Dr. Richard Hynes (M.I.T., MA) for kindly providing the $\alpha 5$ KO mice used in this study and Michael Maniskas for his assistance with the behavioral testing.

Declaration of conflicting interests

The author(s) declared no potential conflicts of interest with respect to the research, authorship, and/or publication of this article.

Authors' contributions

JR and GJB conceptualized and designed the study. JR performed the in vivo experiments/analyzed the data and LdH performed the in vitro experiments/analyzed the data while GJB provided overall oversight of the research. All authors critically reviewed the manuscript and approved the final manuscript as submitted.

References

1. Kahle MP and Bix GJ. Successfully climbing the “STAIRS”: Surmounting failed translation of experimental ischemic stroke treatments. *Stroke Res Treat* 2012; 2012: 374098.
2. del Zoppo GJ, Sharp FR, Heiss WD, et al. Heterogeneity in the penumbra. *J Cereb Blood Flow Metab* 2011; 31: 1836–1851.
3. del Zoppo GJ and Milner R. Integrin-matrix interactions in the cerebral microvasculature. *Arterioscler Thromb Vasc Biol* 2006; 26: 1966–1975.
4. Huvencers S, Truong H and Danen HJ. Integrins: signaling, disease, and therapy. *Int J Radiat Biol* 2007; 83: 743–751.
5. Hynes RO. Integrins: versatility, modulation, and signaling in cell adhesion. *Cell* 1992; 69: 11–25.
6. Yang Y and Rosenberg GA. Blood-brain barrier breakdown in acute and chronic cerebrovascular disease. *Stroke* 2011; 42: 3323–3328.
7. Bolton SJ, Anthony DC and Perry VH. Loss of the tight junction proteins occludin and zonula occludens-1 from cerebral vascular endothelium during neutrophil-induced blood-brain barrier breakdown in vivo. *Neuroscience* 1998; 86: 1245–1257.
8. Dore-Duffy P. Pericytes: pluripotent cells of the blood brain barrier. *Curr Pharm Des* 2008; 14: 1581–1593.
9. Willis CL, Nolan CC, Reith SN, et al. Focal astrocyte loss is followed by microvascular damage, with subsequent repair of the blood-brain barrier in the apparent absence of direct astrocytic contact. *Glia* 2004; 45: 325–337.

10. Baeten KM and Akassoglou K. Extracellular matrix and matrix receptors in blood-brain barrier formation and stroke. *Dev Neurobiol* 2011; 71: 1018–1039.
11. Huber JD, Egleton RD and Davis TP. Molecular physiology and pathophysiology of tight junctions in the blood-brain barrier. *Trends Neurosci* 2001; 24: 719–725.
12. Osada T, Gu YH, Kanazawa M, et al. Interendothelial claudin-5 expression depends on cerebral endothelial cell-matrix adhesion by beta(1)-integrins. *J Cereb Blood Flow Metab* 2011; 31: 1972–1985.
13. Francis SE, Goh KL, Hodivala-Dilke K, et al. Central roles of alpha5beta1 integrin and fibronectin in vascular development in mouse embryos and embryoid bodies. *Arterioscler Thromb Vasc Biol* 2002; 22: 927–933.
14. Goh KL, Yang JT and Hynes RO. Mesodermal defects and cranial neural crest apoptosis in alpha5 integrin-null embryos. *Development* 1997; 124: 4309–4319.
15. Yang JT, Rayburn H and Hynes RO. Embryonic mesodermal defects in alpha 5 integrin-deficient mice. *Development* 1993; 119: 1093–1105.
16. Bix GJ. Perlecan domain V therapy for stroke: a beacon of hope? *ACS Chem Neurosci* 2013; 4: 370–374.
17. Lee B, Clarke D, Al Ahmad A, et al. Perlecan domain V is neuroprotective and proangiogenic following ischemic stroke in rodents. *J Clin Invest* 2011; 121: 3005–3023.
18. Clarke DN, Al Ahmad A, Lee B, et al. Perlecan domain V induces VEGf secretion in brain endothelial cells through integrin alpha5beta1 and ERK-dependent signaling pathways. *PLoS One* 2012; 7: e45257.
19. Al-Ahmad AJ, Lee B, Saini M, et al. Perlecan domain V modulates astrogliosis in vitro and after focal cerebral ischemia through multiple receptors and increased nerve growth factor release. *Glia* 2011; 59: 1822–1840.
20. Li L, Liu F, Welser-Alves JV, et al. Upregulation of fibronectin and the alpha5beta1 and alphavbeta3 integrins on blood vessels within the cerebral ischemic penumbra. *Exp Neurol* 2012; 233: 283–291.
21. van der Flier A, Badu-Nkansah K, Whittaker CA, et al. Endothelial alpha5 and alphav integrins cooperate in remodeling of the vasculature during development. *Development* 2010; 137: 2439–2449.
22. Li L, Welser-Alves J, van der Flier A, et al. An angiogenic role for the alpha5beta1 integrin in promoting endothelial cell proliferation during cerebral hypoxia. *Exp Neurol* 2012; 237: 46–54.
23. Hasan MR, Herz J, Hermann DM, et al. Visualization of macroscopic cerebral vessel anatomy—a new and reliable technique in mice. *J Neurosci Methods* 2012; 204: 249–253.
24. Stroke Therapy Academic Industry R. Recommendations for standards regarding preclinical neuroprotective and restorative drug development. *Stroke* 1999; 30: 2752–2758.
25. Stoeltzing O, Liu W, Reinmuth N, et al. Inhibition of integrin alpha5beta1 function with a small peptide (ATN-161) plus continuous 5-FU infusion reduces colorectal liver metastases and improves survival in mice. *Int J Cancer* 2003; 104: 496–503.
26. Sandoval KE and Witt KA. Blood-brain barrier tight junction permeability and ischemic stroke. *Neurobiol Dis* 2008; 32: 200–219.
27. Du C, Hu R, Csernansky CA, et al. Very delayed infarction after mild focal cerebral ischemia: a role for apoptosis? *J Cereb Blood Flow Metab* 1996; 16: 195–201.
28. Weston RM, Jones NM, Jarrott B, et al. Inflammatory cell infiltration after endothelin-1-induced cerebral ischemia: histochemical and myeloperoxidase correlation with temporal changes in brain injury. *J Cereb Blood Flow Metab* 2007; 27: 100–114.
29. Benedek A, Moricz K, Juranyi Z, et al. Use of TTC staining for the evaluation of tissue injury in the early phases of reperfusion after focal cerebral ischemia in rats. *Brain Res* 2006; 1116: 159–165.
30. Milner R, Hung S, Erokwu B, et al. Increased expression of fibronectin and the alpha 5 beta 1 integrin in angiogenic cerebral blood vessels of mice subject to hypobaric hypoxia. *Mol Cell Neurosci* 2008; 38: 43–52.
31. Kasirer-Friede A, Kahn ML and Shattil SJ. Platelet integrins and immunoreceptors. *Immunol Rev* 2007; 218: 247–264.
32. Loeser RF. Integrins and cell signaling in chondrocytes. *Biorheology* 2002; 39: 119–124.
33. Veine DM, Yao H, Stafford DR, et al. A D-amino acid containing peptide as a potent, noncovalent inhibitor of alpha5beta1 integrin in human prostate cancer invasion and lung colonization. *Clin Exp Metastasis*. Epub ahead of print 25 January 2014. DOI: 10.1007/s10585-013-9634-1.